Laser and Particle Beams (2011), *29*, 11–16.

doi:10.1017/S0263034610000674

Effect of target composition on proton acceleration by intense laser pulses in the radiation pressure acceleration regime

K.H. PAE, I.W. CHOI, AND J. LEE
Advanced Photonics Research Institute, GIST, Buk-gu, Gwangju, Korea
(RECEIVED 8 June 2010; ACCEPTED 22 October 2010)

Abstract

The characteristics of high energy protons generated from thin carbon-proton mixture targets *via* circularly polarized intense laser pulses are investigated using two-dimensional particle-in-cell simulations. It is found that the density ratio n between protons and carbon ions plays a key role in determining the acceleration dynamics. For low n values, the protons are mainly accelerated by the radiation pressure acceleration mechanism, resulting in a quasi-monoenergetic energy spectrum. The radiation pressure acceleration mechanism is enhanced by the directed-Coulomb-explosion of carbon ions which gives a high proton maximum energy, though a large energy spread, for high n values. From a proton acceleration point of view, the role of heavy ions is very important. The fact that the proton energy spectrum is controllable based on the target composition is especially useful in real experimental environments.

Keywords: Laser-plasma interaction; PIC simulation; Proton acceleration

INTRODUCTION

Recently, the use of circularly polarized (CP) intense short laser pulses for generating high energy ions has attracted a great deal of interest because of their potential to generate high-energy quasi-monoenergetic ion beams (Macchi *et al.*, 2005; Yan *et al.*, 2008; Robinson *et al.*, 2008; Rykovanov *et al.*, 2008; Klimo *et al.*, 2008; Henig *et al.*, 2009). CP laser pulses have advantages over linearly polarized laser pulses, such as electron heating suppression, which makes it possible to generate high-quality proton beams from thin targets. In appropriate conditions, a CP laser pulse can be used for the so-called radiation pressure acceleration (RPA) of ions. In this regime, a thin target may be accelerated as a whole *via* the radiation pressure of a laser pulse, resulting in quasi-monoenergetic ions.

However, when multidimensional effects are considered, the RPA mechanism suffers from instabilities (Pegoraro & Bulanov, 2007; Chen *et al.*, 2008). To avoid these stability problems, the generation of high-quality protons/ions from thin foils *via* CP laser pulses through the RPA mechanism has been actively studied through multidimensional particle-in-cell (PIC) simulations. A specially shaped foil target with a transversely varying thickness (Chen *et al.*, 2009) and a density-modulated foil target with a Gaussian density profile in transverse direction (Yu *et al.*, 2009) were proposed to generate GeV collimated quasi-monoenergetic ion beams at an intensity of 10^{22} W/cm^2. Nano-structured double-layer targets were proposed to generate a high-quality proton beam *via* ultra-intense CP laser pulses (Bin *et al.*, 2009; Grech *et al.*, 2009). And an enhanced RPA mechanism was identified, resulting in a GeV collimated proton beam with a 7×10^{21} W/cm^2 intensity laser pulse having a large spot size being produced from a thin target (Yan *et al.*, 2009).

From a practical point of view, targets are composed of multi-species ions in a real experimental environment; as such, the role of heavy ions should be taken into account. In the RPA mechanism, only the ions located in the electron compression layer are bunched and accelerated by the radiation pressure. Moreover, when a target has a low density second layer at the rear side of the target, the ions in the second layer accelerate through the same mechanism (Macchi *et al.*, 2009). Here, we model a realistic target (plastic or diamond-like carbon foil with contaminants) based on a carbon-proton (C-H) mixture target. Basically, a C-H mixture target behaves similar to a thin double layer target; in the early stage of the RPA process, protons move faster than

Address correspondence and reprint requests to: J. Lee, Advanced Photonics Research Institute, GIST, 261 Cheomdan-gwagiro, Buk-gu, Gwangju 500-712, Korea. E-mail: leejm@gist.ac.kr

heavy ions to form an additional layer between the electron layer and the remaining heavy ions. Through a series of two-dimensional (2D)-PIC simulations, we then investigate the effect of target composition on proton acceleration using CP laser pulses in an RPA regime. The main findings in the present paper are that there are two main mechanisms of proton acceleration from thin C-H mixture targets. In addition, it is found that proton acceleration dynamics can be controlled by changing a single parameter of the target composition $n = n_{\mathrm{p}}/n_{\mathrm{C}}$, where n_{p} and n_{C} are the number densities of the protons and carbon ions, respectively.

SIMULATION PARAMETERS

In this study, we used the 2D version of the ALPS code, which is an explicit electromagnetic PIC code for laser-plasma interaction simulations based on fully second-order algorithms. A CP laser pulse has a Gaussian spatial profile, with a spot size $w_0 = 16\lambda$ full width at half maximum (FWHM) and a flattop temporal profile of $20\lambda/c$ duration with $1\lambda/c$ ramps for both rising and falling sides, where λ is the laser wavelength, and c is the speed of light in a vacuum. The laser pulse intensity is then given by a normalized vector potential $a_0 = 50$, which corresponds to $I\lambda_{\mu}^2 = 6.85 \times 10^{21}$ W/(cm^{2}μm^2). The pulse is normally incident on a fully ionized C-H mixture target initially located at a position $x = 5\lambda$. The thin C-H mixture target is modeled using a thin plasma slab composed of carbon ions (C^{6+}), protons, and electrons. The rest mass of carbon ions is set to $m_{\mathrm{C}} = 12m_{\mathrm{p}}$, where m_{p} is the proton rest mass; the target electron density is fixed at $n_{\mathrm{e}} = 400n_{\mathrm{c}}$, where n_{c} is the critical density, in a manner that both $n_e = const. = n_p + 6n_C$ and $n_p = n \times n_C$ are satisfied simultaneously. Furthermore, the target thickness is set at $d \approx \lambda/25$, which corresponds to the "optimal" RPA condition (Macchi *et al.*, 2009),

$$\pi \frac{n_e}{n_c} \frac{d}{\lambda} \approx a_0.$$

Note that the full extraction of electrons from a thin target requires a smaller target thickness (or higher intensity) than that of the optimal RPA condition. Here, the size of the simulation domain is $45\lambda \times 48\lambda$ in the (x, y) directions, respectively. The grid cell size is $\lambda/200$ in both directions, and 720 electron macro-particles per cell were used. Here, all the boundaries absorb incoming fields and particles. By the absorbing boundaries, incoming electromagnetic fields are absorbed to avoid spurious reflections, and simulation particles going out of the simulation domain are removed from the simulation.

SIMULATION RESULTS AND DISCUSSION

The temporal evolution of the density of electrons, protons, and carbon ions for the $n = 0.1$ case is shown in Figure 1. The whole target, including protons and carbon ions, was then accelerated by the RPA mechanism as a single layer. This result is similar to Macchi *et al.* (2009), in which a

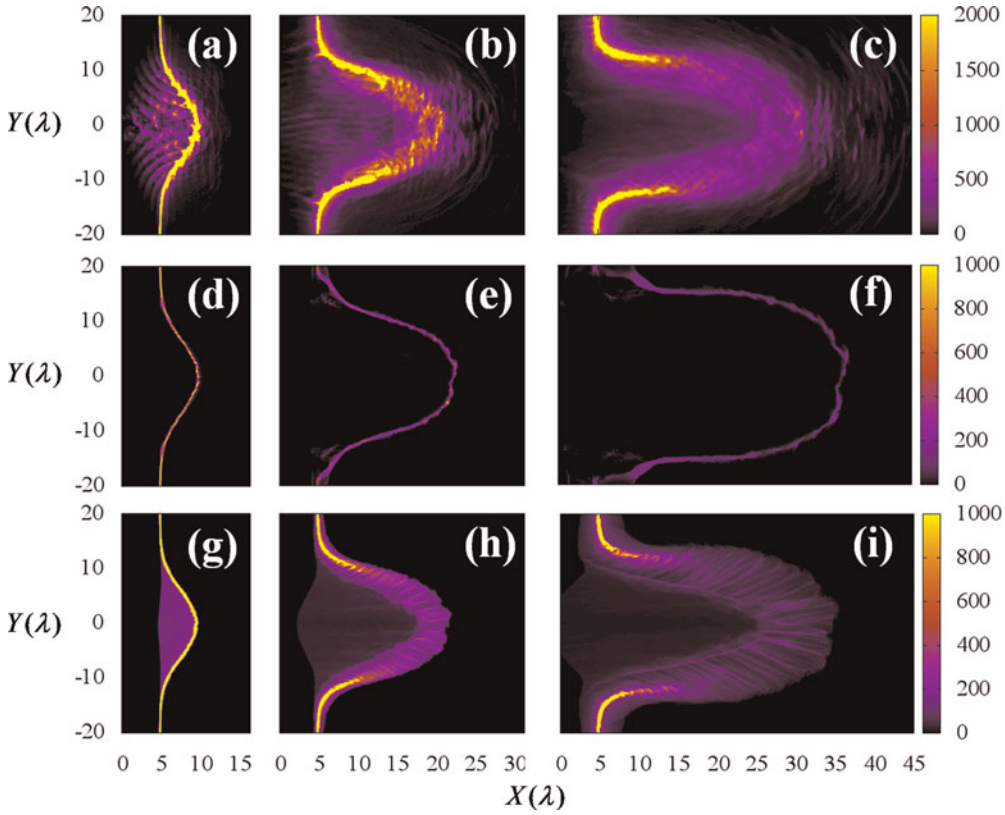

Fig. 1. (Color online) The temporal evolution of electrons ((**a**)–(**c**)), protons ((**d**)–(**f**)), and carbon ions ((**g**)–(**i**)) for $n = 0.1$ case at times $t = 43$ fs ((**a**),(**d**),(**g**)), $t = 103$ fs ((**b**),(**e**),(**h**)), and $t = 163$ fs ((**c**),(**f**),(**i**)) after the start of laser-target interaction. The laser pulse is incident from the left and hits the target initially located at $x = 5\lambda$. Color bars (grayscales) are in arbitrary units.

https://doi.org/10.1017/S0263034610000674 Published online by Cambridge University Press

double layer target was used in a one-dimensional simulation. In our simulation, however, electrons were distributed over the full region of the accelerated layer rather than maintained in a thin compression layer. We attribute the longitudinal broadening of the electron layer to the breaking of the balance between radiation pressure and charge separation force. The carbon ions were slowly accelerated by the radiation pressure because of the relatively higher charge per mass ratio and lower mobility than those of the protons. Most of the electrons were trapped by the carbon ions *via* the charge separation force, which kept the RPA process stable. Nevertheless, because only the ions located in the electron compression layer were accelerated by the radiation pressure, the thickness of the carbon ion layer broadened. Furthermore, a portion of the high energy electrons were pushed out of the main acceleration region by the radiation pressure, as can be seen in Figures 1a–1c. These processes caused longitudinal broadening of the electron layer; due to this longitudinal broadening, the reflectivity of the laser field decreased, thereby reducing the RPA efficiency at later times. This is clearly identified in by comparing Figure 2 with Figure 1. The laser pulse electric field still accelerating electrons at $t = 103$ fs and it continues to later times. In Figure 2c, however, a significant portion of the laser pulse leaked out of the electron cloud to the forward direction, which means a lower RPA efficiency after the time $t = 103$ fs. Also, a significant amount of carbon ions is accelerated by the RPA mechanism as well as protons.

Because of the relatively small proton number, however, the effects of the electrons spread on the thickness of the proton layer were not significant. Hence, the thickness of the proton layer does not significantly increase with time, resulting in a quasi-monoenergetic energy spectrum. In contrast, the thickness of the carbon ion layer does increase with time, up to about 10λ, because of its relatively high density. From Figures 1f and 1i, we expect the maximum energy of carbon ions per nucleon to be similar to the central energy of protons. In this case, the normal RPA is the dominant mechanism of both proton and carbon ion acceleration. The electron cloud covers both protons and carbon ions. Due to the relatively higher charge concentration of carbon ions, maximum electron density is located in the carbon ion cloud.

The Rayleigh-Taylor type instabilities (RTI) (Pegoraro & Bulanov, 2007) set on in the early stage due to the Gaussian spatial profile of the laser pulse. However, due to the relatively low proton density, effects of RTI on the proton acceleration are not significant.

The temporal evolution of the target for the $n = 12$ case is shown in Figure 3. Due to the relatively higher mobility and higher charge per mass ratio of protons than for the carbon ions, protons are predominantly accelerated by the charge separation force in a short time; the protons in the central region are mainly accelerated by the RPA mechanism, and carbon ions follow slowly. Most electrons move in step with protons, forming a so-called self-organized double layer. After a short interaction period, carbon ions are no longer accelerated by the electrostatic field, because of the field screening effect by the proton layer and by the relatively long distance between the leading electrons and carbon ions. Consequently, the central region of the proton layer separates from carbon ions at an early stage, clearly identified in a comparison of Figures 3d and 3g. As a result, the carbon ion core remains behind the electron-proton double layer. In Figures 3g–3i, the carbon ion core is seen to experience a directed-Coulomb-explosion (DCE) (Bulanov *et al.*, 2008) due to the excess positive charges. In a DCE, ions expand predominantly in the longitudinal direction. The expansions of protons and carbon ions are shown in Figure 4. Carbon ions expand symmetrically with respect to the longitudinally moving expansion front and a significant number of them reside at the expansion front. As can be seen in Figure 4b, the expansion of the protons shows the DCE effect clearly.

After the onset of DCE, protons in the central region are further accelerated by the DCE-enhanced RPA mechanism. During DCE, carbon ions push nearby protons *via* repulsive force while pulling nearby electrons. Thus, DCE alters the force balance condition and results in a broad electron layer in the longitudinal direction. Because the charge density of protons is dominant over carbon ions, in contrast to the $n = 0.1$ case, broadening of the electron distribution directly causes the corresponding proton layer to broaden.

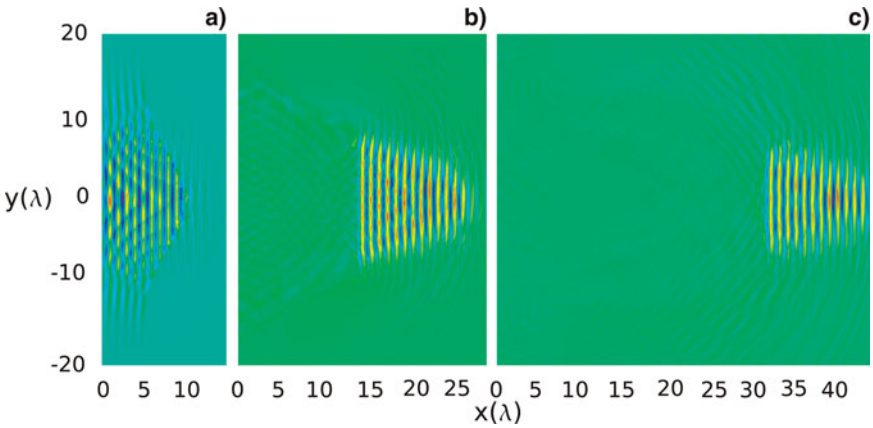

Fig. 2. (Color online) The temporal evolution of the electric field y-component for $n = 0.1$ case at times $t = 43$ fs (**a**), $t = 103$ fs (**b**), and $t = 163$ fs (**c**).

https://doi.org/10.1017/S0263034610000674 Published online by Cambridge University Press

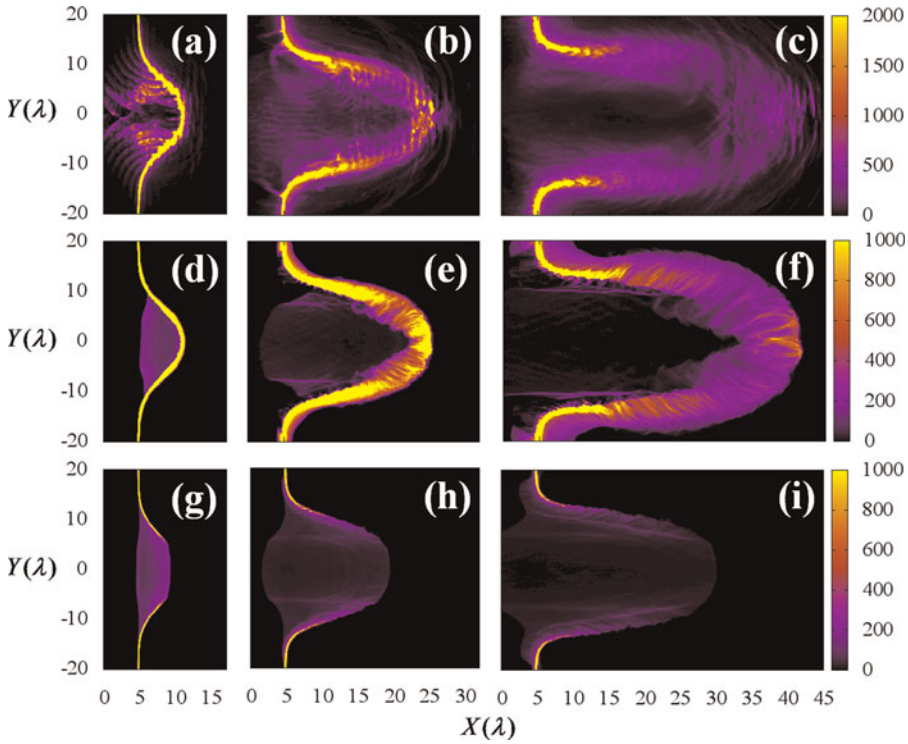

Fig. 3. (Color online) The same as in Figure 1, except $n = 12$.

This in turn may cause the large energy spread in the proton energy spectrum.

The role of carbon ions in this case is to enhance the maximum proton energy *via* the DCE and to increase the proton energy spread. Also, due to the relatively high proton density, RTI significantly affects the accelerated protons in the side region, as can be seen in Figures 3e and 3f.

These scenarios were subsequently confirmed by the temporal evolution of the maximum proton energy. In Figure 5, the temporal evolutions of the maximum proton energy for the $n = 0.1$ and $n = 12$ cases are compared with the result of the one-dimensional analytic model of (Tripathi *et al.*, 2009) for an electron-proton target. Here, t_L is the laser period. For the $n = 0.1$ case, evolution of the maximum proton energy in the early stage ($t < 18t_L$, 60 fs after the start of laser-target interaction) is similar to the theoretical curve. This means that in the early stage, the target is accelerated as a whole by the radiation pressure. After time $t \approx 18t_L$, however, the electrons spread by breaking the longitudinal balance between the radiation pressure and the charge separation force, as mentioned above. This spread causes a field leakage of the laser pulse and results in a lower acceleration gradient than the theoretical curve at later times.

On the other hand, for the high n case, protons are accelerated to high energy in a very short time scale by the radiation pressure. In the central region, only the protons are accelerated by the radiation pressure and carbon ions undergo the DCE process. Furthermore, the effect of the longitudinal electron spread and the RTI on the highest energy protons is not significant, as can be seen from Figures 3c and 3f. The protons-only acceleration by the DCE-enhanced RPA mechanism results in a high acceleration gradient.

To investigate the effect of target composition in greater detail, we then varied n while keeping other parameters constant. The energy spectra at time $t = 49t_L$ from a series of 2D-PIC simulations are shown in Figure 6, in which

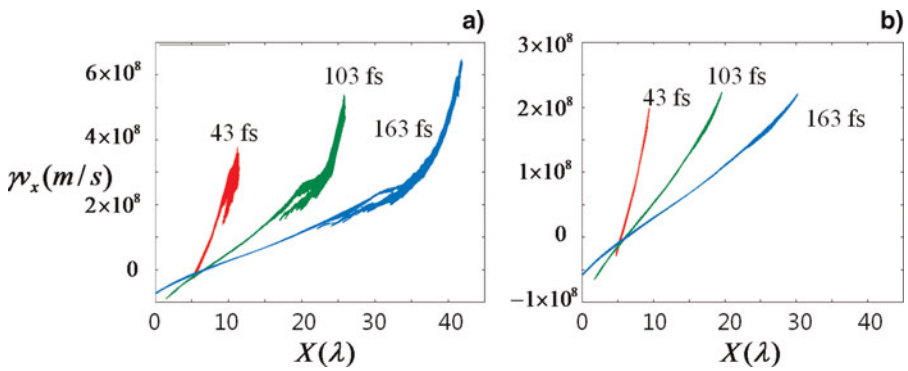

Fig. 4. (Color online) The temporal evolution of the γv_x-x phase spaces of protons (**a**) and carbon ions (**b**) for $n = 12$ case. Only macroparticles within central radius $R < 5\lambda$ are shown.

https://doi.org/10.1017/S0263034610000674 Published online by Cambridge University Press

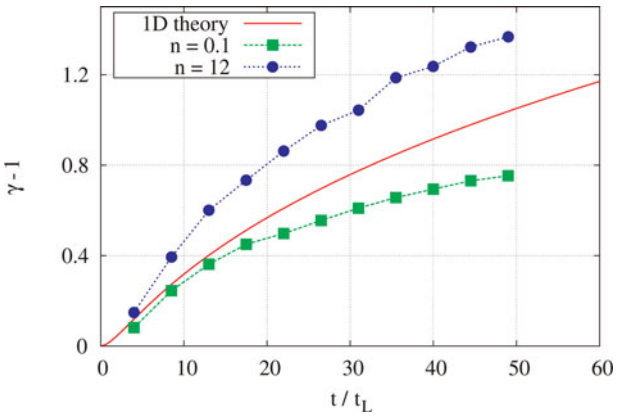

Fig. 5. (Color online) The temporal evolution of the maximum proton energy. t_L is the laser period. The theoretical curve is calculated by the formula in Tripathi *et al.* (2009).

only protons within a central radius $R < 5\lambda$ were selected for the graphs. The figure shows that for the $n = 0.1$ case, the maximum proton energy is about 700 MeV and the FWHM energy spread is about 12%; in low n ($n < 1$) cases, proton energy spectra are quasi-monoenergetic. Furthermore, the $n = 0.1$ and $n = 0.5$ cases have a similar maximum energy. In these cases, the energy spread increases with increasing n, suggesting that the lowness of n is important for monoenergetic proton generation. This posits is analogous to a double layer target having a thin low density second layer driven by a linearly polarized intense laser pulse (Esirkepov *et al.*, 2002). A similar result was also observed in a target-normal sheath acceleration regime (Robinson *et al.*, 2006).

In the high n (n, 1) cases, there is a dramatic change in the shapes of the proton energy spectra, compared to the spectra in the low n cases. Furthermore, the maximum proton energy increases to over 1 GeV, and the maximum proton energy increases with increasing n. For the $n = 6$ case, electrons are not fully extracted from the carbon ion core region due to the high carbon ion concentration. In addition, the carbon ions are partially accelerated by the RPA mechanism; as a result, the DCE of the carbon ions is weaker than that of the $n = 12$ case in spite of the higher initial carbon ion density, thereby suggesting that DCE is supplementary to the RPA mechanism. For the electron-proton compound target (not shown in the figure), the maximum proton energy was similar to that of the $n = 6$ case. This trend implies that there is an optimum value of n for maximum proton energy. It was also noted that the proton energy spectra of the high n cases have a large energy spread due to the breaking of the longitudinal force balance; as a result, the average proton energy is similar to that of the low n cases. Therefore, the main difference between our result and the result in Robinson *et al.* (2006) is that the maximum proton energy does not increase monotonously with increasing n in the RPA regime. This difference is due to the difference of the acceleration mechanism, target-normal sheath acceleration, and DCE-enhanced RPA.

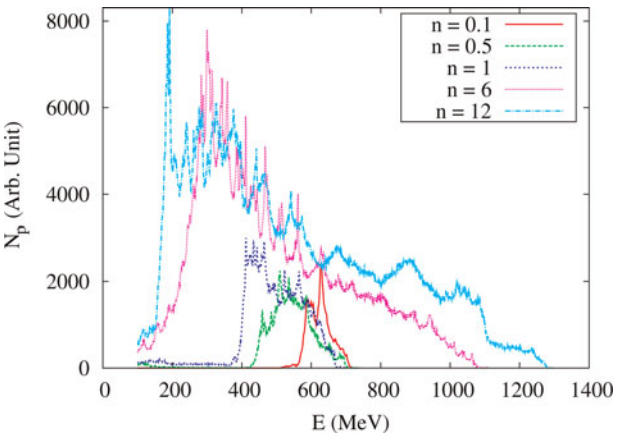

Fig. 6. (Color online) The energy spectra of protons at time $t = 49t_L$ for various n. Only protons within central radius $R < 5\lambda$ are selected for the graphs.

CONCLUSION

In summary, we identified two dynamics of proton accelerations from thin C-H mixture targets *via* intense CP short laser pulses. Proton accelerations can be categorized by a single parameter of the target composition $n = n_p/n_C$, the density ratio between protons and carbon ions. For low n (<1.0) values, quasi-monoenergetic high energy protons are primarily generated through the normal RPA mechanism. It was shown here that the RPA mechanism enhanced by DCE produces GeV energy protons, albeit those having a large energy spread for high n (1.0) values, thereby implying that the proton energy spectrum can be controlled by the single parameter n. In the overall proton acceleration process, the role of carbon ions was found to be different for low n and high n values. For low n values, carbon ions reduced the RPA efficiency, whereas it enhanced the maximum proton energy *via* DCE for high n values. Therefore, this study suggests that the role of heavy ions should be taken into account in a real experimental environment, and that the control of proton energy spectrum *via* target composition may be very useful for future investigations in this area.

In this regime, a single layer target with multiple ion species and double layer target show similar behavior, as mentioned in the Introduction. So, n-optimized targets can be realized by using ultra-thin double layer target or hydrogen doped ultrathin target. For example, a diamond-like carbon containing H (hydrogenated amorphous carbon, a-C:H) or a polymer coated ultrathin target.

ACKNOWLEDGEMENTS

This work was supported by the Ministry of Knowledge and Economy of Korea through the Ultrashort Quantum Beam Facility Program.

https://doi.org/10.1017/S0263034610000674 Published online by Cambridge University Press

REFERENCES

Bin, J.H., Lei, A.L., Yang, X.Q., Huang, L.G., Yu, M.Y., Yu, W. & Tanaka, K.A. (2009). Quasi-monoenergetic proton beam generation from a double-layer solid target using an intense circularly polarized laser. *Laser Part. Beams* **27**, 485–490.

Bulanov, S.S., Brantov, A., Bychenkov, V.Yu., Chvykov, V., Kalinchenko, G., Matsuoka, T., Rousseau, P., Reed, S., Yanovsky, V., Litzenberg, D.W., Krushelnick, K. & Maksimchuk, A. (2008). Accelerating monoenergetic protons from ultrathin foils by flat-top laser pulses in the directed-Coulomb-explosion regime. *Phys. Rev. E* **78**, 026412.

Chen, M., Pukhov, A., Sheng, Z.M. & Yan, X.Q. (2008). Laser mode effects on the ion acceleration during circularly polarized laser pulse interaction with foil targets. *Phys. Plasmas* **15**, 113103.

Chen, M., Pukhov, A., Yu, T.P. & Sheng, Z.M. (2009). Enhanced collimated GeV monoenergetic ion acceleration from a shaped foil target irradiated by a circularly polarized laser pulse. *Phys. Rev. Lett*. **103**, 024801.

Esirkepov, T.Zh., Bulanov, S.V., Nishihara, K., Tajima, T., Pegoraro, F., Khoroshkov, V.S., Mima, K., Daido, H., Kato, Y., Kitagawa, Y., Nagai, K. & Sakabe, S. (2002). Proposed double-layer target for the generation of high-quality laser-accelerated ion beams. *Phys. Rev. Lett*. **89**, 175003.

Grech, M., Skupin, S., Nuter, R., Gremillet, L. & Lefebvre, E. (2009). High-quality ion beams by irradiating a nanostructured target with a petawatt laser pulse. *New J. Phys*. **11**, 093035.

Henig, A., Steinke, S., Schnüer, M., Sokollik, T., Hörlein, R., Kiefer, D., Jung, D., Schreiber, J., Hegelich, B.M., Yan, X.Q., Meyer-Ter-Vehn, J., Tajima, T., Nickles, P.V., Sandner, W. & Habs, D. (2009). Radiation-pressure acceleration of ion beams driven by circularly polarized laser pulses. *Phys. Rev. Lett*. **103**, 245003.

Klimo, O., Psikal, J., Limpouch, J. & Tikhonchuk, V.T. (2008). Monoenergetic ion beams from ultrathin foils irradiated by ultrahigh-contrast circularly polarized laser pulses. *Phys Rev. ST Accel. Beams*. **11**, 031301.

Macchi, A., Cattani, F., Liseykina, T.V. & Cornolti, F. (2005). Laser acceleration of ion bunches at the front surface of overdense plasmas. *Phys. Rev. Lett*. **94**, 165003.

Macchi, A., Veghini, S. & Pegoraro, F. (2009). "Light Sail" acceleration reexamined. *Phys. Rev. Lett*. **103**, 085003.

Pegoraro, F. & Bulanov, S.V. (2007). Photon bubbles and ion acceleration in a plasma dominated by the radiation pressure of an electromagnetic pulse. *Phys. Rev. Lett*. **99**, 065002.

Robinson, A.P.L., Bell, A.R. & Kingham, R.J. (2006). Effect of target composition on proton energy spectra in ultraintense laser-solid interactions. *Phys. Rev. Lett*. **96**, 035005.

Robinson, A.P.L., Zepf, M., Kar, S., Evans, R.G. & Bellei, C. (2008). Radiation pressure acceleration of thin foils with circularly polarized laser pulses. *New J. Phys*. **10**, 013021.

Rykovanov, S.G., Schreiber, J., Meyer-Ter-Vehn, J., Bellei, C., Henig, A., Wu, H.C. & Geissler, M. (2008). Ion acceleration with ultra-thin foils using elliptically polarized laser pulses. *New J. Phys*. **10**, 113005.

Tripathi, V.K., Liu, C.S., Shao, X., Eliasson, B. & Sagdeev, R.Z. (2009). Laser acceleration of monoenergetic protons in a self-organized double layer from thin foil. *Plasma Phys. Contr. Fusion* **51**, 024014.

Yan, X.Q., Lin, C., Sheng, Z.M., Guo, Z.Y., Liu, B.C., Lu, Y.R., Fang, J.X. & Chen, J.E. (2008). Generating high-current monoenergetic proton beams by a circularly polarized laser pulse in the phase-stable acceleration regime. *Phys. Rev. Lett*. **100**, 135003.

Yan, X.Q., Wu, H.C., Sheng, Z.M., Chen, J.E. & Meyer-Ter-Vehn, J. (2009). Self-organizing GeV, nanocoulomb, collimated proton beam from laser foil interaction at 7×10^{21} W/cm^2. *Phys. Rev. Lett*. **103**, 135001.

Yu, T.P., Chen, M. & Pukhov, A. (2009). High quality GeV proton beams from a density-modulated foil target. *Laser Part. Beams* **27**, 611–617.

https://doi.org/10.1017/S0263034610000674 Published online by Cambridge University Press